

Subcellular proteomic approach for identifying the signaling effectors of protein kinase C- β_2 under high glucose conditions in human umbilical vein endothelial cells

MIN ZHANG^{1*}, FANG SUN^{2*}, FANGFANG CHEN¹, BO ZHOU¹, YAQIAN DUAN¹, HONG SU¹ and XUEBO LIN¹

¹Department of Endocrinology, The First Affiliated Hospital of Chongqing Medical University, Chongqing 400016; ²Department of Hypertension and Endocrinology, Daping Hospital, Third Military Medical University, Chongqing 400042, P.R. China

Received November 13, 2014; Accepted August 5, 2015

DOI: 10.3892/mmr.2015.4403

Abstract. The high glucose-induced activation of protein kinase C- β_2 (PKC- β_2) has an essential role in the pathophysiology of diabetes-associated vascular disease. In the present study, human umbilical vein endothelial cells (HUVECs) were cultured in high and normal glucose conditions prior to being infected with a recombinant adenovirus to induce the overexpression of PKC- β_2 . The activity of PKC- β_2 was also decreased using a selective PKC- β_2 inhibitor. A series of two-dimensional electrophoresis images detected ~800 spots in the nuclei, and ~600 spots in the cytosol. Following intra- and inter-group cross-matching, 38 significantly altered spots were identified as high glucose-induced and PKC- β_2 -associated nuclear proteins. In addition to the observation that the regulation of key proteins involved in the nuclear factor (NF)- κ B signaling cascade occurred in the cytosol, various transcription factors, including peroxisome proliferator-activated receptor δ (PPAR- δ), were also altered in the nuclei. A human protein-protein interaction network of potential connections of PKC- β_2 -associated proteins was

constructed in the proteomics investigation using Biological General Repository for Interaction Datasets. The results indicated that PKC- β_2 may be involved in high glucose-induced glucose and lipid crosstalk by regulating PPAR- δ . In addition, NF- κ B inhibitor-interacting Ras-like protein 1 may be important in the PKC- β_2 -NF- κ B inhibitor-NF- κ B signaling pathway in HUVECs under high-glucose conditions.

Introduction

Diabetes mellitus is a common and increasing public health concern, which affects developed and developing countries. In China, the prevalence of diabetes and pre-diabetes were estimated to be 9.7 and 15.5%, respectively, in 2008 (1). Although diabetic vascular disease contributes significantly to the disability and mortality rates of diabetic patients, the mechanisms underlying its pathology remain to be fully elucidated. Previous studies confirmed that the earliest hallmark for the development of such complications is endothelial cell injury (2,3) characterized by increased cell inflammation and leukocyte-endothelial cell adhesion, and by alterations in cell proliferation, cell cycle, cellular metabolism and cell differentiation (4-6). There are four major molecular damage signaling pathways, which are considered indicative of a diabetic condition: Increases in the activity of the polyol pathway, increases in the formation of advanced glycation end products, increases in the activation of the diacylglycerol-protein kinase C (PKC) signaling pathway and increases in the production of reactive oxygen species (7).

PKC is a widely conserved family, containing ≥ 12 serine-threonine kinases, which are involved in a number of complex cell regulatory events. The functions of the individual PKC isoforms are conferred by their subcellular localization, their differentially regulated cofactor-dependent activity and their signaling architecture following translocation and activation (8,9). Among the diverse PKC isoforms, PKC- β_2 and PKC- δ are preferentially activated in the heart and vasculature (10,11). The functional role and mechanism of PKC- β_2 are important, specifically in diabetes. In previous years, several cellular signaling pathways associated with the PKC- β_2 isoform have been uncovered. Studies in Zucker fatty

Correspondence to: Dr Bo Zhou, Department of Endocrinology, The First Affiliated Hospital of Chongqing Medical University, 1 Youyi Road, Yuzhong, Chongqing 400016, P.R. China
E-mail: zhoubo915@126.com

*Contributed equally

Abbreviations: PKC, protein kinase C; DAG, diacylglycerol; HUVECs, human umbilical vein endothelial cells; MALDI-TOF-MS, matrix-assisted laser desorption/ionization time-of-flight tandem mass spectrometry; NF- κ B, nuclear factor- κ B; MAPK, mitogen-activated protein kinase; CDC7, cell division cycle 7; HSP7E, heat shock 70 kDa protein 14; PPAR- δ , peroxisome proliferator-activated receptor δ ; NKIRAS1, NF- κ B inhibitor-interacting Ras-like protein 1

Key words: protein kinase C- β_2 , subcellular proteomic approach, vein endothelial cells

rats and in mice overexpressing PKC- β_2 in the vasculature indicated that PKC- β_2 upregulates the production of nitric oxide and the expression of endothelial nitric oxide synthase via the Akt signaling pathway (12). In human umbilical vein endothelial cells (HUVECs) exposed to high glucose, the mRNA expression levels of vascular endothelial growth factor and vascular cell adhesion molecule 1 increase via the PKC- β_2 activation-dependent peroxisome proliferator-activated receptor (PPAR)- α signaling pathway (13). In cultured cardiomyocytes from neonatal Sprague-Dawley rats treated with high glucose, the structure and function of PKC- β_2 are significantly affected by the PKC/nuclear factor (NF)- κ B/c-Fos signaling pathway (14). In human aortic vascular smooth muscle cells, alterations in cell adhesion, cell speed and lamellipodia formation appear to be affected by the PKC- β_2 -phosphoinositide 3-kinase signaling pathway (15). The majority of the above-mentioned studies have focused on only one molecule or signaling pathway. However, cell signaling cascades are not linear, but are complex and involve crosstalks. Global characterization of the mechanism underlying the signaling pathway of the PKC- β_2 isoform remains to be fully elucidated.

In the present study, a combination of recombinant adenovirus transfection, subcellular fraction extraction, two-dimensional electrophoresis (2-DE), mass spectrometry and signaling network analysis was used to identify novel downstream effectors of the PKC- β_2 signaling pathway, and to examine crosstalk between the nucleus and cytoplasm in high glucose-stimulated HUVECs. The present study also used subcellular and functional proteomics to determine effective techniques to profile subcellular signaling in endothelial cells during PKC- β_2 activation. These findings may provide system-wide insight into the mechanisms underlying diabetes-associated blood vessel damage.

Materials and methods

Cell culture and experimental groups. HUVECs were provided by the Institute of Biological Sciences of Chongqing Medical University (Chongqing, China). The cells were cultured in RPMI-1640 medium (Gibco Life Technologies, Carlsbad, CA, USA) supplemented with 10% fetal bovine serum (Gibco Life Technologies) at 37°C in an atmosphere containing 5% CO₂ and 95% air. To ameliorate cell responsiveness to high glucose, the cells were serum starved for 24 h prior to experimentation. For the 2-DE analysis, the HUVECs were divided into the following four groups: Normal glucose control group (NG), comprising cells treated with 5.6 mmol/l D-glucose (Bio Basic Canada, Inc., Markham, ON, Canada); high glucose group (HG), comprising cells treated with 25 mmol/l D-glucose; PKC- β_2 overexpression group (PO), comprising cells transfected with Ad5-PKC- β_2 cultured in medium containing 25 mmol/l glucose; empty vector control group (EV), comprising cells transfected with Ad5-Null, cultured in medium containing 25 mmol/l glucose. Ad5-PKC- β_2 and Ad5-Null were constructed and identified according to the protocol of previous studies by our group (16,17). For western blot analyses, a PKC- β_2 inhibition group (POPI), comprising cells transfected with Ad5-PKC- β_2 cultured in medium containing 25 mmol/l glucose and

1 μ mol/l CGP 53353 (Sigma-Aldrich, St. Louis, MO, USA); a high glucose and PKC- β_2 inhibition group (HGPI), comprising cells cultured in medium containing 25 mmol/l glucose and 1 μ mol/l CGP 53353; and a normal glucose and PKC- β_2 inhibition group (NGPI) comprising cells cultured in medium containing 5.6 mmol/l glucose and 1 μ mol/l CGP 53353, were also included. All cells were cultured for six days following plating.

Recombinant adenovirus infection of HUVECs. The recombinant adenoviral vector constructed to express PKC- β_2 had a titer of 7.5×10^9 U/ml Ad5-PKC- β_2 . The cells were seeded into 6-well culture plates (1.5×10^4 cells/well) and treated with RPMI-1640 medium supplemented with 25 mmol/l glucose. The cells were grown until they were in a logarithmic phase and washed twice with serum-free RPMI 1640 medium. The recombinant adenovirus, which was constructed to express PKC- β_2 at a multiplicity of infection (MOI) of 100, was then added to each well. After 90 min, the medium was replaced with RPMI-1640 medium supplemented with 5.6 mmol/l or 25 mmol/l glucose and 10% fetal bovine serum. Ad5-Null was used as an empty vector to infect cells, which served as a control. Over the following 6 days, the medium was replaced every 2 days. These cells were used for subsequent proteomics analysis and confocal imaging assays.

Subcellular fractionation: Nuclear and cytoplasm protein extraction.

Nuclear extraction and purification. The nuclear extraction and purification process was performed, as previously described by Turck *et al.* (18), with modifications. Cell suspensions were centrifuged at $1,000 \times g$ for 10 min at 4°C. Following discarding of the supernatant, the cell pellet was resuspended ($\sim 1 \times 10^6$ /ml) in lysis buffer (Keygen Biotech, Jiangsu, China) containing 5 mM MgCl₂, 10 mM NaCl, 5 mM Tris-HCl (pH 7.5), 1 mM dithiothreitol (DTT) and 1 mM phenylmethanesulfonyl fluoride, prior to being placed on ice for 10 min. This step was repeated twice. The nuclear pellet was resuspended in 0.25 M sucrose solution. The nuclei were then layered on a 2 M sucrose solution and centrifuged for 30 min at $30,000 \times g$ at 4°C. To precipitate the DNA, 10 mM spermine (Keygen Biotech) was added for 1 h at room temperature. To extract the protein, the nuclei were placed three times into liquid nitrogen (Jingfeng Co., Sichuan, China) and centrifuged at $12,000 \times g$ for 30 min; the supernatant containing the nuclear proteins was collected. Protein concentrations were quantified using an RC DC protein assay kit (Bio-Rad Laboratories, Inc., Hercules, CA, USA), and the protein solutions were aliquoted (500 μ l per tube).

Cytosol protein extraction. The cytosol protein was extracted using a ProteoExtract Cytosol/Mitochondria Fraction kit (Merck Millipore, Darmstadt Germany), according to the manufacturer's instructions. The cells were collected by centrifugation at $600 \times g$ for 5 min at 4°C, prior to being washed with 10 ml ice-cold phosphate-buffered saline (PBS) and centrifuged at $600 \times g$ for 5 min at 4°C. The supernatant was then discarded, and the cells were resuspended ($\sim 1 \times 10^6$ /ml) with 1 ml 1X Cytosol Extraction Buffer mix containing DTT and protease inhibitors. The cell suspension was incubated on ice for 10 min and then homogenized on ice using an ice-cold

dounce tissue grinder (Keygen Biotech). The homogenates were transferred into a 1.5 ml microcentrifuge tube and centrifuged at 700 x g for 10 min at 4°C. The supernatants were then transferred into a fresh 1.5 ml tube and centrifuged at 10,000 x g for 30 min at 4°C. The resulting supernatant, the cytosolic fraction, was collected and the samples were stored at -80°C. Protein concentrations were quantified using a Bio-Rad RC DC protein assay kit (Bio-Rad Laboratories, Inc.), and the protein solutions were aliquoted (500 µl per tube).

2-DE and image analysis. The protein samples (180 µg nuclear protein, 200 µg cytosol protein) were applied to ReadyStrip™ immobilized pH gradient strips (17 cm; pH 3-10; nonlinear; Bio-Rad Laboratories, Inc.) using a passive rehydration method as follows: The protein samples were added to rehydration buffer (final volume, 400 µl), and 1% (w/v) DTT and ampholytes were added prior to use. Then ReadyStrip IPG strips [pH 3-10, 17 cm, unlined (Bio-Rad Laboratories)] were soaked in the rehydration buffer and covered with mineral oil to be passively rehydrated for 14 h at 17°C. Following rehydration, the strips were transferred to a PROTEAN® i12™ Isoelectric Focusing (IEF) system (Bio-Rad Laboratories, Inc.). IEF was performed as follows: 250 V for 30 min, linear; 1,000 V for 1 h, rapid; linear ramping to 10,000 V for 6 h; and 10,000 V for 6 h. Once IEF was complete, the strips were equilibrated in equilibration buffer (Keygen Biotech), containing 25 mM Tris-HCl (pH 8.8), 6 M urea, 20% glycerol, 2% SDS and 130 mM DTT) for 15 min at room temperature, prior to being incubated in the same buffer containing 200 mM iodoacetamide (Keygen Biotech) instead of DTT for an additional 15 min. The second dimension was separated using a 12% SDS-PAGE gradient at 60 V for 30 min followed by 200 V for 7 h at 16°C. For the 2-DE analysis, each of the paired samples was run in triplicate to ensure the consistency of the data. The protein spots were visualized with silver nitrate (Merck Millipore). The differentially expressed proteins were identified using PDQuest Image Analysis Software 9.0 (Bio-Rad Laboratories, Inc.). The quantity of each spot in a gel was normalized as a percentage of the total quantity of all spots in that gel, and was evaluated in terms of optical density. Only the spots that changed consistently and significantly (>1.5-fold) were selected for tandem mass spectrometry (MS/MS) analysis.

Matrix-assisted laser desorption/ionization time of flight (MALDI-TOF)-MS analysis and identification

Tryptic in-gel digestion. Protein spots of interest were excised from the gel using a sterile blade and washed three times with MilliQ water (Merck Millipore). The gel spots were destained twice with 0.2 ml 100 mM NH₄HCO₃ in 50% acetonitrile (ACN) for 45 min at 37°C prior to being dehydrated in 100% ACN for 5 min. The spots were then incubated with 10 µl of 10 µg/ml trypsin (Bio-Rad Laboratories, Inc.) at room temperature for 1 h, followed by incubation at 37°C overnight in 20 µl digestion buffer (40 mM NH₄HCO₃ in 10% ACN; Keygen Biotech). The liquid was then removed. The tryptic peptides were extracted twice using 50 µl of 50% ACN with 5% trifluoroacetic acid (TFA; Keygen Biotech) by sonication (JY98-IIIN; Ningbo Scientz Biotechnology Co., Ltd, Zhejiang, China) for 15 min. All extracts were then pooled and dried in a Speed Vac (Keygen Biotech) at room temperature. The

peptides were desalted using C18 Zip Tips (EMD Millipore, Billerica, MA, USA) and reconstituted in 5 µl 70% ACN with 0.1% TFA.

Protein identification and database search. The MALDI-TOF-MS data were compared against the *Homo sapiens* subset of sequences, according to the following parameters: Enzyme, trypsin; allowance of up to one missed cleavage peptide; mass tolerance, 1.0 Da; parameter carbamoyl methylation (Cys); variable modification parameters, oxidation (at Met) and phosphorylation (ST), peptide summary report. The data were analyzed using the MASCOT search engine (Matrix science, London, UK; <http://www.matrixscience.com>) against the Swiss-Prot protein database. The proteins were identified on the basis of two or more peptides, whose ion scores exceeded the threshold and were P<0.05, indicating a 95% confidence interval for the matched peptides.

Western blot analysis. Total protein was extracted using lysis buffer containing a protease inhibitor cocktail. The nuclear and cytosolic proteins were previously prepared and stored at -80°C. For western blot analysis, 20 µg protein was separated by 12% SDS-PAGE, transferred to a polyvinylidene difluoride membrane (EMD Millipore), prior to being probed separately with goat polyclonal anti-phosphorylated (p)-PKC-β₂ (cat. no. sc-11760; 1:500; Santa Cruz Biotechnology, Inc., Dallas, TX, USA), mouse monoclonal anti-PPAR-δ (cat. no. ab58137; 1:170; Abcam, Cambridge, UK) or mouse monoclonal anti-NF-κB inhibitor-interacting Ras-like protein 1 (NKIRAS1; cat. no. ab13666; 1:750; Abcam) primary antibodies. The primary antibodies were incubated overnight at 4°C and then incubated with horseradish peroxidase-conjugated secondary antibodies (cat. no. ab150115; 1:2,000; Abcam) 2 h at 37°C. The blots were then visualized using an Enhanced Chemiluminescence detection kit (Beyotime Institute of Biotechnology, Jiangsu, China). A Bio-Rad gel imaging system (Bio-Rad Laboratories) was used to capture images of the gels and the optical density values of the bands were determined using Quantity One image software (Bio-Rad Laboratories). The relative expression levels of target proteins were represented by the ratio of target protein bands to β-actin.

Immunofluorescence and confocal microscopy. The cells (~1x10⁶/ml) were cultured in six-well culture plates with a glass cover slip (10 mm diameter) at the bottom of each well of the seven groups: NG, HG, PO, NGPI, HGPI, POPI and EV. On the seventh day, the cells were treated as follows: Medium was removed from each well, the cells were washed three times with PBS, treated with 4% paraformaldehyde (EMD Millipore) for 15 min and washed again with PBS in the dark. The cells were subsequently permeabilized with 0.2% Triton-X 100 (Solarbio, Beijing, China) for 10 min in the dark. Following three washes with PBS, the cells were blocked with 1% goat serum and 0.1% bovine serum albumin (Sigma-Aldrich) in PBS for 60 min at room temperature. An anti-NF-κB (p65/RELA) antibody (EMD Millipore) was diluted to 1:100 in blocking solution (Keygen Biotech) and added to each cover slip overnight at 4°C. The cover slips were washed with PBS. Fluorescein isothiocyanate (FITC)-conjugated goat anti-rabbit IgG (1:160) in blocking

solution was added to each cover slip, and the cover slips were incubated in the dark at 37°C for 1.5 h. The cover slips were washed three times with PBS and mounted with 50% glycerol (Sigma-Aldrich). The fluorescence intensity of p65/RELA in the nuclei and cytosol was detected at an excitation wavelength of 488 nm using a FITC filter (Leica Microsystems, Oberkochen, Germany). The average absolute fluorescence intensities of the labeled p65/RELA were calculated using Image-Pro Plus 6.0 (Media Cybernetics, Rockville, MD, USA). The obtained fluorescence intensity images were analyzed using the average fluorescence as a quantitative parameter.

Cell cycle assays. Following incubation in culture medium for six days, the cells were harvested by trypsinization (HyClone, Logan, UT, USA), resuspended in PBS at a concentration of 1×10^5 cells/ml and fixed in ice-cold 75% ethanol (30 min at 4°C). The cells were then washed twice in cold PBS, treated with 20 μ g/ml RNase A (HyClone) for 30 min at room temperature, and stained with 50 μ g/ml propidium iodide (PI; Keygen Biotech). Finally, the cells were resuspended in 1 ml PBS and analyzed using flow cytometry, according to the manufacturer's instructions.

Apoptosis assays. The rates of apoptosis were measured using an Annexin V-FITC Cell Apoptosis kit (Abcam, Cambridge, MA, USA). To measure early or late/necrotic apoptotic cell death, $\sim 1.5 \times 10^5$ cells were stained with 5 μ l FITC-labeled Annexin V and PI in 500 μ l binding buffer (Keygen Biotech). The cells were then analyzed using flow cytometry, according to the manufacturer's instructions. Annexin V and PI emissions were detected in the FL1 and FL2 channels of a FACSCalibur flow cytometer (BD Biosciences, Franklin Lakes, NJ, USA) using emission filters of 488 nm and 532 nm, respectively.

Web-based protein-protein interactions (PPIs). To identify the PPIs, the web-based protein information sharing software tool, the Biological General Repository for Interaction Datasets (BioGRID 3.1) was used. A PPI network was constructed of the potential connections for the PKC- β_2 -associated proteins, which were identified in the proteomics investigation.

Statistical analysis. The data are expressed as the mean \pm standard deviation. The 2-DE quantitative comparisons were performed using PDQuest gel analysis software 9.0 (Bio-Rad Laboratories, Inc.). The spot volumes were expressed as numerical values of optical density. Student's *t*-test was used for independent groups and inter-group comparisons. The data from the apoptosis and cell cycle assays were analyzed using one-way analysis of variance, and a Student-Newman-Keuls test was used for further comparisons between the two groups. All statistical analyses were performed using SPSS 11.0 (SPSS, Inc. Chicago, IL, USA). $P < 0.05$ was considered to indicate a statistically significant difference.

Results

Effectiveness of recombinant adenovirus transfection of HUVECs at MOI 100 and the role of a selective PKC- β_2 inhibitor on p-PKC- β_2 . In the present study, an overexpressing

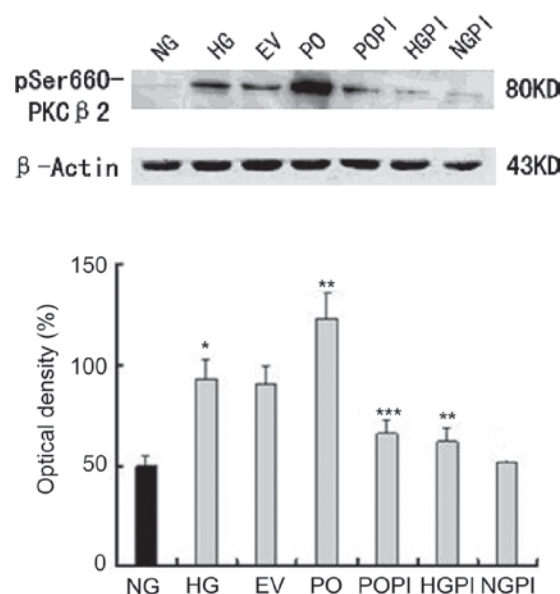


Figure 1. Functional analysis of the effectiveness of recombinant adenovirus transfection of HUVECs at a multiplicity of infection of 100. The phosphorylation levels of PKC- β_2 in the HUVECs was assessed using western blotting, and the following groups were analyzed: Normal glucose control group (5.6 mmol/l glucose); high glucose group (25 mmol/l glucose); empty vector control group (25 mmol/l glucose+Ad5-null); PKC- β_2 overexpression group (25 mmol/l glucose+Ad5-PKC- β_2); PKC- β_2 inhibition group (25 mmol/l glucose+Ad5-PKC- β_2 +1 μ mol/l CGP53353); high glucose inhibition group (25 mmol/l glucose+1 μ mol/l CGP53353); normal glucose inhibition group (5.6 mmol/l glucose+1 μ mol/l CGP53353). The data are expressed as the mean \pm standard deviation. * $P < 0.05$, vs. NG group; ** $P < 0.05$, vs. HG group; *** $P < 0.05$, vs. PO group ($n=5$). HUVECs, human umbilical vein endothelial cells; PKC- β_2 , protein kinase C- β_2 ; NG, normal glucose group; HG, high glucose group; EV, empty vector group; PO, PKC- β_2 overexpression group; POPI, PKC- β_2 inhibition group; HGPI, high glucose inhibition group; NGPI, normal glucose inhibition group.

PKC- β_2 cell model was constructed using a recombinant adenoviral vector, which was designed to express PKC- β_2 . The cells were transfected at an MOI of 100; Ad5-Null was used as an empty vector to infect the cells, which served as a control. Western blotting with antibodies targeting PKC- β_2 phosphorylated at specific residues revealed that incubating the cells with high glucose levels increased the phosphorylation of Ser-660 in the HUVECs. Treatment with CGP53353 (1 μ mol/l), a selective PKC- β_2 inhibitor, significantly affected the basal expression levels of p-PKC- β_2 under high glucose conditions (25 mmol/l). As shown in Fig. 1, incubation of the HUVECs in medium containing high glucose concentration levels (25 mmol/l) resulted in a significant increase in the phosphorylation levels of PKC- β_2 (1.87-fold), compared with the NG group ($n=5$; $P < 0.05$). Similar results were observed in cells transfected with Ad5-null under high glucose conditions, however, no significant changes were observed, despite the empty vector effect, between the HG and EV groups (Fig. 1). Furthermore, the protein expression levels of PKC- β_2 in the cells PO group were markedly increased (1.32-fold), compared with the HG group ($P < 0.05$). Treating the cells with the selective PKC- β_2 inhibitor, CGP53353, prevented the glucose-induced and overexpression-induced phosphorylation of PKC- β_2 ($P < 0.05$), compared with the HG group and PO group. The levels of p-PKC- β_2 were unchanged, compared with those observed under normal glucose conditions following the inactivation of PKC- β_2 by CGP53353.

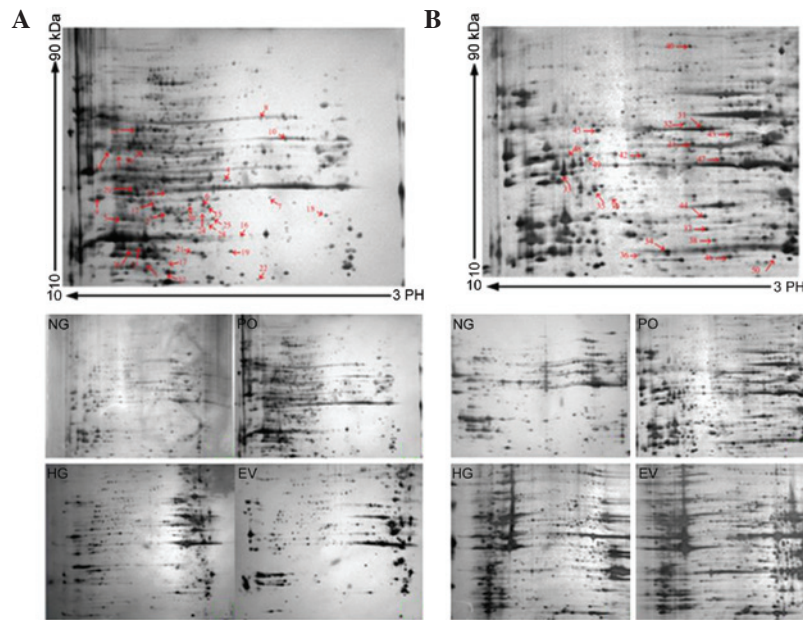


Figure 2. (A) 2-DE gel of the nuclear proteins from the HUVECs of each group. Nuclear proteins (180 μ g) were separated on pH 3-10 nonlinear IPG strips (17 cm) in the first dimension, prior to being separated by 12% SDS-PAGE in the second dimension and visualized by silver staining. The HUVECs were divided into four treatment groups: Normal glucose control group (5.6 mmol/l glucose); high glucose group (25 mmol/l glucose); PKC- β_2 overexpression group (Ad5-PKC- β_2 +25 mmol/l glucose); empty vector control group (Ad5-Null+25 mmol/l glucose). A total of 30 differentially expressed spots were identified using MALDI-TOF-MS/MS (marked with arrows and numbers). (B) 2-DE gel of the cytoplasmic proteins from the HUVECs of each group. Cytoplasmic proteins (200 μ g) were separated on pH 3-10 nonlinear IPG strips (17 cm) in the first dimension, prior to being separated by 12% SDS-PAGE in the second dimension and visualized by silver staining. The treatment groups were the same as those in Fig. 2A. A total of 20 differentially expressed spots were identified using MALDI-TOF-MS/MS (marked with arrows and numbers). Information on each numbered spot is reported in Table I. 2-DE, two-dimensional electrophoresis; HUVECs, human umbilical vein endothelial cells; MALDI-TOF-MS/MS, matrix-assisted laser desorption/ionization-time of flight-tandem mass spectrometry; IPG, immobilized pH gradient; PKC- β_2 , protein kinase C- β_2 . NG, normal glucose group; HG, high glucose group; EV, empty vector group; PO, PKC- β_2 overexpression group.

Comparison of nuclear and cytoplasmic protein expression levels in HUVECs, determined using 2-DE. Representative 2-DE maps of the four groups are shown in Fig. 2. To ensure reproducibility, the experiment was repeated three times for each group, and the same protein patterns were obtained. The evaluation, normalization of images and compensation of background variations were performed using PDQuest gel analysis software 9.0. An average of 812 ± 28 spots in the NG group, 832 ± 27 spots in the HG group, 843 ± 31 spots in the EV group and 864 ± 36 spots in the PO group were visualized for the nuclear proteins. For the cytosol protein samples, an average of 591 ± 32 spots in the NG group, 662 ± 27 spots in the HG group, 624 ± 21 spots in the EV group and 637 ± 32 spots in the PO group were visualized. Protein expression levels in the gels under the various conditions were quantified and processed for comparison, and a >1.5 -fold difference in optical density between groups was considered statistically significant. To screen the protein spots with differential expression in the various conditions, a three-step comparison was performed. The 2-DE images of the nuclear proteins from the cells under normal glucose conditions were compared with those of the cells under high glucose conditions. Inter-group statistical analyses allowed the detection of 47 ± 6 protein spots from the nucleus. The protein spots exhibiting differential expression were considered to be induced by high glucose stress. To screen the altered protein spots induced by PKC- β_2 activation, inter-group cross-matching was applied between the Ad5-PKC δ -transfected group and the Ad5-null-transfected group cultured in 25 mmol/l glucose medium, resulting in 52 ± 5 spots. The protein spots exhibiting differential expression were

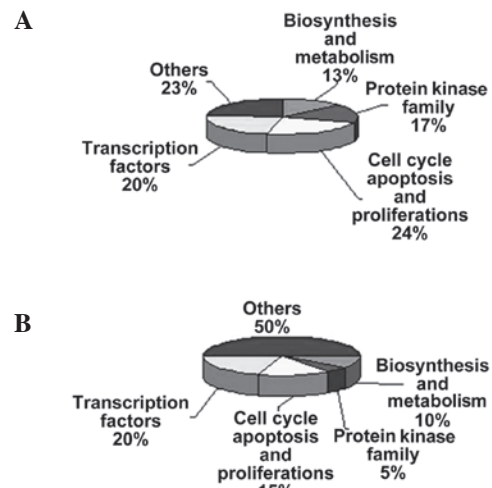


Figure 3. A total of 50 identified proteins were functionally classified into five groups. (A) Nuclear proteins identified in the HUVECs were involved in biosynthesis and metabolism (13%); protein kinase family members (17%); cell cycle, apoptosis and proliferation (24%); transcription factors (23%); or other functions (23%). (B) Cytoplasmic proteins identified in the HUVECs were involved in biosynthesis and metabolism (10%); protein kinase family members (5%); cell cycle, apoptosis and proliferation (15%); transcription factors (20%); or other functions (50%). HUVECs, human umbilical vein endothelial cells.

considered to be induced by sustained PKC- β_2 activation under high glucose stress. A total of 38 common protein spots from steps one and two were defined as PKC- β_2 -associated proteins

Table I. Proteins identified by matrix-assisted laser desorption/ionization time of flight/mass spectrometry in the nuclear and cytoplasm of human umbilical vein endothelial cells.

Spot and function	Symbol	Protein name	SWISS-PORT accession no.	Molecular mass (kD)	Theoretical PI	Queries matched	Sequence coverage (%)	Upregulation or downregulation
Subcellular location: Nucleus								
Biosynthesis and metabolism								
1	DUS22	Dual specificity protein phosphatase 22	Q9NRW4	21.19	8.28	4	18	U (1.56±0.05 fold)
2	DYR	Dihydrofolate reductase	P00374	29.11	7.63	8	32	U (1.60±0.03 fold)
3	CP2U1	Cytochrome P450, family 2, subfamily U, polypeptide 1	Q7Z499	62.41	8.63	3	25	U (1.69±0.10 fold)
4	1A1L1	1-aminocyclopropane-1-carboxylate synthase-like protein	Q96Q16	57.86	6.01	2	19	D (1.59±0.08 fold)
Protein kinase family								
5	PRKACB	cAMP-dependent protein kinase catalytic subunit beta	P22694	40.71	8.84	4	27	U (1.62±0.04 fold)
6	MAPK3	Mitogen-activated protein kinase 3	P27361	43.48	6.86	7	37	U (1.65±0.04 fold)
7	AMPK β1	5'-AMP-activated protein kinase subunit beta-1	Q9Y478	30.53	5.49	3	24	U (1.71±0.12 fold)
8	PRK CZ	Protein kinase C zeta type	Q05113	68.55	5.49	8	12	U (1.57±0.02 fold)
9	MP2K7	Dual specificity mitogen-activated protein kinase kinase 7	O14733	47.91	9.26	5	18	U (1.65±0.12 fold)
Cell cycle, apoptosis and proliferation								
10	LMNB2	Lamin-B2	Q03252	67.76	5.29	7	10	U (1.66±0.08 fold)
11	THAP1	THAP domain-containing protein 1	Q9NVV9	25.44	8.66	4	28	U (1.55±0.03 fold)
12	CCNE	G ₁ /S-specific cyclin-E2	O96020	47.3	7.96	5	32	U (1.65±0.07 fold)
13	DBF4B	Protein DBF4 homolog B	Q8NFT6	68.57	8.72	5	25	U (1.67±0.10 fold)
14	CDC7	Cell division cycle 7-RELATED protein kinase	O00311	64.65	8.96	3	27	D (1.60±0.05 fold)
15	CCNJ	Cyclin-J	Q5T5M9	43.238	6.75	6	19	D (1.56±0.04 fold)
16	PHB	Prohibitin	P35232	29.84	5.75	4	13	D (1.66±0.03 fold)
Transcription factors								
17	SAP25	Histone deacetylase complex subunit	Q8TEE9	21.21	7.63	8	38	U (1.64±0.06 fold)
18	RCAN3	Calcipressin-3	Q9UKA8	27.77	4.54	9	61	U (1.60±0.04 fold)

Table I. Continued.

Spot and function	Symbol	Protein name	SWISS-PORT accession no.	Molecular mass (kDa)	Theoretical PI	Queries matched	Sequence coverage (%)	Upregulation or downregulation
19	COMD7	COMM domain-containing protein 7	Q86VX2	22.7	5.96	8	56	U (1.74±0.09 fold)
20	ZN193	Zinc finger protein 193	O15535	46.95	6.95	4	7	U (1.60±0.07 fold)
21	EID2	EP300-interacting inhibitor of differentiation	Q8N6L1	25.29	6.95	7	42	U (1.61±0.07 fold)
22	ATRAP	Type-1 angiotensin II receptor-associated protein	Q6RW13	17.58	5.71	3	11	D (1.57±0.03 fold)
23	PPARD	Peroxisome proliferator activated receptor Δ	Q03181	50.683	7.53	8	56	D (1.82±0.06 fold)
Others								
24	CAH2	Carbonic anhydrase 2	P00918	29.26	6.87	13	21	U (1.66±0.05 fold)
25	GLNA	Glutamine synthetase	P15104	42.67	6.43	15	23	U (1.61±0.07 fold)
26	GSTA1	Glutathione-S-transferase A1	P08263	25.67	8.91	16	24	U (1.58±0.02 fold)
27	PPIGA	Cyclophilin A	Q13427	18.23	7.68	12	31	U (1.57±0.04 fold)
28	GON4L	GON4L protein	Q6PHZ4	34.33	6.52	2	6	U (1.58±0.04 fold)
29	FIBB	Fibrinogen β chain	P02675	56.56	8.64	7	22	U (1.69±0.10 fold)
30	HNRPL	Heterogeneous nuclear ribonucleoprotein L	P14866	64.73	8.46	2	18	U (1.62±0.10 fold)
Subcellular location: Cytoplasm								
Biosynthesis and metabolism								
31	UAP1	UDP-N-acetylglucosamine pyrophosphorylase	Q16222	59.13	5.92	9	26	U (1.61±0.02 fold)
32	HSP7E	Heat-shock 70kDa protein 14	Q0VDF9	55.44	5.41	6	29	D (1.74±0.05 fold)
Protein kinase family								
33	PRKACA	cAMP-dependent protein kinase catalytic subunit α	P17621	40.68	8.84	5	8	U (1.63±0.02 fold)
CC, apoptosis and proliferation								
34	BNIP3	BCL2/adenovirus E1B 19kDa interacting protein 3	Q12983	21.53	6.31	5	12	U (1.60±0.04 fold)
35	NEK6	Serine/threonine-protein kinase Nek6	Q9HC98	36.26	8.26	4	7	U (1.74±0.06 fold)
36	CDN1B	Cyclin-dependent kinase inhibitor 1B	P46527	22.29	6.54	3	23	D (1.64±0.03 fold)

Table I. Continued.

Spot and function	Symbol	Protein name	SWISS-PORT accession no.	Molecular mass (kD)	Theoretical PI	Queries matched	Sequence coverage (%)	Upregulation or downregulation
Transcription factors								
37	NRBF2	Nuclear receptor binding factor	Q96F24	32.53	5.61	4	24	U (1.72±0.07 fold)
38	NKIRAS1	NF-κB inhibitor-interacting Ras-like protein 1	Q9NYS0	22.80	6.00	6	28	D (1.66±0.13 fold)
39	ACOT8	Acyl-coenzyme A thioesterase 8	O14734	36.35	7.23	2	10	D (1.60±0.04 fold)
40	SAPMI	Sterile alpha and TIR motif containing 1	Q6SZW1	80.365	6.14	7	9	D (1.61±0.04 fold)
Others								
41	TBG1	Tubulin, gamma 1	P23258	51.48	5.75	6	14	U (1.68±0.10 fold)
42	ACTT1	Actin-RELATED protein T1	Q8TDG2	42.24	6.32	5	9	U (1.58±0.06 fold)
43	DESM	Mutant desmin	P17661	53.53	5.21	7	16	U (1.67±0.04 fold)
44	F92A1	Protein FAM92A1	A1XBS5	33.59	5.89	3	18	U (1.67±0.11 fold)
45	LCAP	Leucine aminopeptidase	Q9UIQ6	56.41	7.58	2	11	U (1.61±0.04 fold)
46	HPCL1	Hippocalcin-like protein 1	P37235	22.29	5.21	7	23	U (1.65±0.05 fold)
47	TXNL1	Thioredoxin-like protein 5	O43396	42.17	5.4	3	12	U (1.58±0.06 fold)
48	UB2CB	Ubiquitin-conjugating enzyme E2C-binding protein	Q7Z6I8	44.61	8.51	4	8	D (1.66±0.12 fold)
49	MIIP	Migration and invasion-inhibitory protein	Q5IXC2	43.37	8.33	4	19	D (1.61±0.09 fold)
50	MLRV	Myosin regulatory light chain 2	P10916	18.78	4.92	5	21	D (1.58±0.07 fold)

U, upregulated; D, downregulated.

Table II. Differently expressed proteins associated with PKC- β_2 and involved in molecular mechanisms in human umbilical vein endothelial cells.

Spot code	Protein name	Protein function	Reference
6	MAPK3	MAPKs are serine-threonine kinases that regulate a wide variety of cellular functions. MAPKs are involved in both the initiation and of meiosis, mitosis, and post-mitotic functions in differentiated cells by phosphorylating several transcription factors.	19
13	DBF4B	DBF4B is a regulatory subunit of CDC7, activating its kinase activity, and has a central role in DNA replication and cell proliferation. DBF4B is required for the progression of the S and M phases. The CDC7-DBF4B complex selectively phosphorylates the MCM2 subunit at Ser-40, and is also involved in regulating the initiation of DNA replication during the cell cycle.	20,21
14	CDC7	CDC7 encodes a cell division cycle protein with kinase activity that is important for the G ₁ /S phase transition.	22,23
23	PPARD	PPARD is a member of the peroxisome proliferator-activated receptor family. PPARD regulates the peroxisomal β -oxidation pathway of fatty acids, and functions as a transcriptional activator for the acyl-coenzyme A oxidase gene. PPARD decreases NPC1L1 expression following ligand activation.	24,25
32	HSP7E	HSP7E inhibits stress-induced JNK activation, thereby reducing apoptosis.	26
38	NKIRAS1	NKIRAS1 is an atypical Ras-like protein that acts as a potent regulator of NF- κ B activity by preventing the degradation of NFKBIB by the majority of signals, which is why NFKBIB is more resistant to degradation. NKIRAS1 may act by inhibiting the phosphorylation of NFKBIB, and by mediating cytoplasmic retention of the p65/RELA NF- κ B subunit. It is unclear whether NKIRAS1 acts as a GTPase. GTP and GDP-bound forms of NKIRAS1 inhibit NFKBIB phosphorylation.	27

MAPK, mitogen-activated protein kinase; DBF4B, protein DBF4 homolog B; CDC7, cell division cycle 7-RELA protein kinase; PPARD, peroxisome proliferator-activated receptor Δ ; NPC1L1, Niemann-Pick C1-like 1; HSP7E, heat-shock 70 kDa protein 14; JNK, c-Jun N-terminal kinase; NF- κ B, nuclear factor- κ B; NKIRAS1, nuclear factor NF- κ B inhibitor-interacting Ras-like protein 1; NFKBIB, NF- κ B inhibitor β ; RELA, v-rel avian reticuloendotheliosis viral oncogene homolog A; GTP, guanosine triphosphate; GDP, guanosine diphosphate.

induced under high glucose stress, determined by inter-group comparison. A total of 30 differentially expressed spots were identified using MALDI-TOF-MS (marked with arrows and numbers in Fig. 2A). For the cytosol protein 2-DE gels, the same process was performed, and 28 common protein spots were identified. From these spots, 20 proteins were identified using MALDI-TOF-MS (marked with arrows and numbers in Fig. 2B). A database search was subsequently performed using peptide mass fingerprints. Using subcellular proteomics, 50 proteins were identified. Information regarding the numbered spots is presented in Tables I and II (19-27). For these spots, the accession number, protein name, molecular mass (kD), theoretical PI, number of peptides, queries matched and sequence coverage for each particular isoform of a protein were reported. The majority of these proteins were found to be involved in cellular functions, including biosynthesis, metabolism, cell cycle, apoptosis, proliferation and transcription, and are associated with the protein kinase family (Fig. 3A and B).

Identification of proteins located downstream of PKC- β_2 using western blot analysis. To determine whether the protein alterations observed in the proteomics analysis correlated with changes in protein expression at the translational level, two proteins, the expression levels of which were significantly altered in the proteomics analysis, PPAR- δ and NKIRAS1 (Figs. 4 and 5), were selected for further examination using western blotting.

Determination of the expression levels of PPAR- δ in the various groups of HUVECs. A PPAR- δ -specific mouse monoclonal antibody was used to quantify the expression levels of PPAR- δ in the nuclear fraction under various conditions. The groups were the same as in Fig. 1. As shown in Fig. 4, there was a 1.2 ± 0.03 -fold increase in the expression levels of PPAR- δ (also termed PPAR- β) in the HUVECs exposed to 25 mmol/l glucose, compared with those exposed to 5 mmol/l glucose ($n=5$; $P<0.05$). In the cells overexpressing

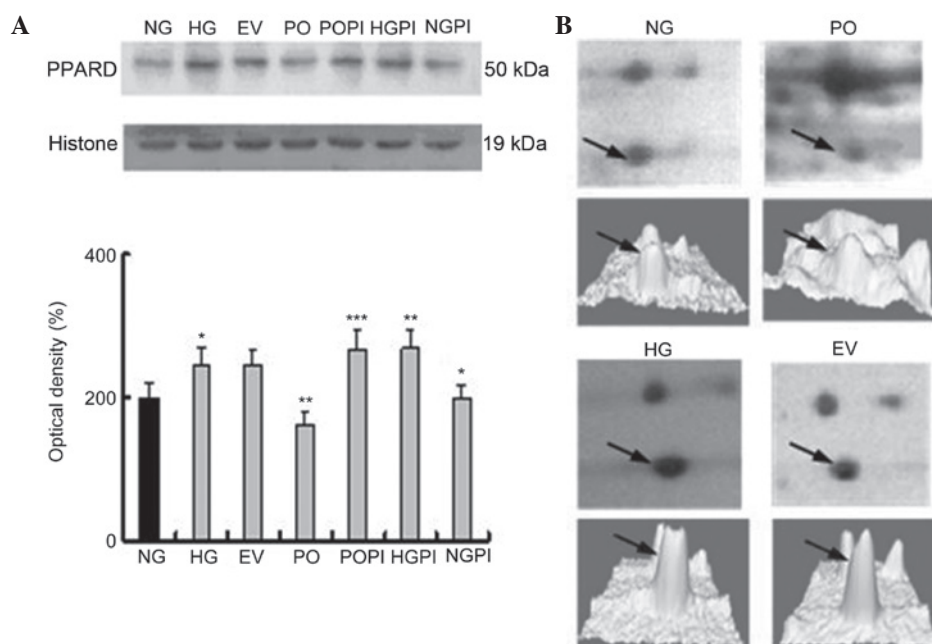


Figure 4. Expression levels of the PKC- β_2 downstream protein, PPAR- δ , in the nuclear fraction. (A) Representative images of the quantitative measurements of the protein expression of PPAR- δ in the seven treatment groups using western blot analysis with a PPAR- δ -specific antibody. The error bars represent the mean \pm standard deviation of the mean. * $P < 0.05$, vs. NG control group; ** $P < 0.05$, vs. HG group; *** $P < 0.05$, vs. PO group ($n = 5$). (B, above) Two-dimensional electrophoresis gel map of PPAR- δ from the nuclear fractions of the NG, HG, EV and PO groups; arrows indicate PPAR- δ spots. (B, below) Three-dimensional image of the expression of PPAR- δ , determined using PDQuest software. PKC- β_2 , protein kinase C- β_2 ; PPAR, peroxisome proliferator-activated receptor; NG, normal glucose group; HG, high glucose group; EV, empty vector group; PO, PKC- β_2 overexpression group; POPI, PKC- β_2 inhibition group; HGPI, high glucose inhibition group; NGPI, normal glucose inhibition group.

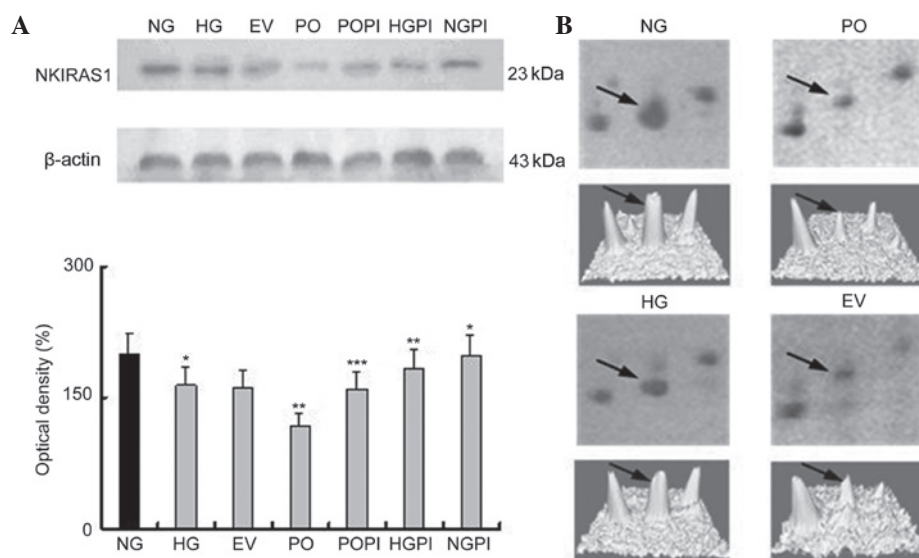


Figure 5. (A) Expression levels of NKIRAS1 in the cytoplasmic fraction, determined using western blot analysis with an NKIRAS1-specific antibody. The error bars represent the mean \pm standard deviation of the mean. * $P < 0.05$, vs. NG control group; ** $P < 0.05$, vs. HG group; *** $P < 0.05$, vs. PO group ($n = 5$). (B, above) Two-dimensional electrophoresis gel map of NKIRAS1 in the nuclear fractions of the NG, HG, EV and PO groups; arrows indicate the NKIRAS1 spots. (B, below) Three-dimensional image of the expression of NKIRAS1, determined using PDQuest software. NKIRAS1, nuclear factor NF- κ B inhibitor-interacting Ras-like protein 1. PKC- β_2 , protein kinase C- β_2 ; NG, normal glucose group; HG, high glucose group; EV, empty vector group; PO, PKC- β_2 overexpression group.

PKC- β_2 in 25 mmol/l glucose, these stimulatory effects were partly eliminated, and the expression was decreased by $34.0 \pm 2.3\%$, compared with the HG group ($P < 0.05$). No significant changes in the expression levels of PPAR- δ were observed in the EV group. Furthermore, treatment of the cells with the selective PKC- β_2 inhibitor, CGP53353 (1 μ mol/l),

led to an increase in the expression of PPAR- δ ($110 \pm 2.4\%$), compared with the HG group ($P < 0.05$; Fig. 4).

Determination of the expression levels of NKIRAS1 in the various groups of HUVECs. An NKIRAS1-specific mouse monoclonal antibody was used to quantify NKIRAS1

expression levels in the cytoplasmic fraction under various conditions. As shown in Fig. 5, incubation of the HUVECs with medium containing high glucose (25 mmol/l) resulted in a decrease in the expression of NKIRAS1 by 17.69%, compared with the NG group ($n=5$; $P<0.05$). No significant changes in the expression of NKIRAS1 were observed, compared with the EV group. Furthermore, the protein expression levels of NKIRAS1 in the cells overexpressing PKC- β_2 in 25 mmol/l glucose were significantly lower, by 28.16%, compared with the HG group ($P<0.05$). Treating the cells with the selective PKC- β_2 inhibitor, CGP53353, inhibited the PKC- β_2 -induced decrease in the expression of NKIRAS1 ($P<0.05$), compared with the HG group and PO group. The expression levels of NKIRAS1 were increased following PKC- β_2 inactivation by CGP53353 (1.12-fold), compared with the HG group, ($P<0.05$), and 1.34-fold, compared with the PO group ($P<0.05$).

Upregulation and nuclear translocation of NF- κ B (p65/RELA) is induced by sustained PKC- β_2 activation under high glucose stress in HUVECs. Protein function analysis offered further insight into the above findings. NKIRAS1 was one of the PKC- β_2 downstream effectors identified in the present study. NKIRAS1 acts as a potent regulator of NF- κ B activity by inhibiting the phosphorylation of NF- κ B and by mediating the cytoplasmic retention of the p65/RELA NF- κ B subunit (27). To determine the role of high glucose levels and PKC- β_2 in a potential HUVEC PKC- β_2 -NF- κ B signaling pathway, immunofluorescence labeling of NF- κ B (p65/RELA) was detected using confocal microscopy and an isoform-specific antibody. As shown in Fig. 6, under basal conditions, p65/RELA exhibited a homogeneous distribution in the cytoplasm of the HUVECs. There was little distribution of p65/RELA in the nucleus under normal glucose conditions (Fig. 6A; NG group). However, the fluorescence intensity per cell was increased in the cytoplasm, and the cytosol-to-nucleus fluorescence ratio was decreased in the presence of high glucose levels (Fig. 6A; HG group). Ad5-null transfection was used as an empty vector control (Fig. 6A; EV group). As expected, no marked differences were observed, and the quantity and distribution of fluorescence were the same in response to the 25 mmol/l high glucose concentrations in the cells transfected with or without the Ad5-null vector. When PKC- β_2 was overexpressed (Fig. 6A; PO group), the fluorescence intensity per cell significantly increased (1.95-fold), compared with the non-transfected HG control group ($**P<0.05$; Fig. 6B). In addition, the cytosol-to-nucleus fluorescence ratio of p65/RELA significantly decreased in these groups (1.21 ± 0.06 and 1.48 ± 0.07 , respectively; $P<0.05$; Fig. 6C). These results suggested that the protein expression levels of p65/RELA in the HUVECs were increased, and that p65/RELA was activated via nuclear translocation following high glucose exposure. Therefore, the upregulation and nuclear translocation of NF- κ B (p65/RELA) were induced by sustained PKC- β_2 activation under high glucose stress in the HUVECs.

Cell cycle analysis. Flow cytometric analysis was used to determine which cell cycle phase was affected by high glucose levels, and whether PKC- β_2 activation affected the HUVECs. The majority of the cells were distributed in the

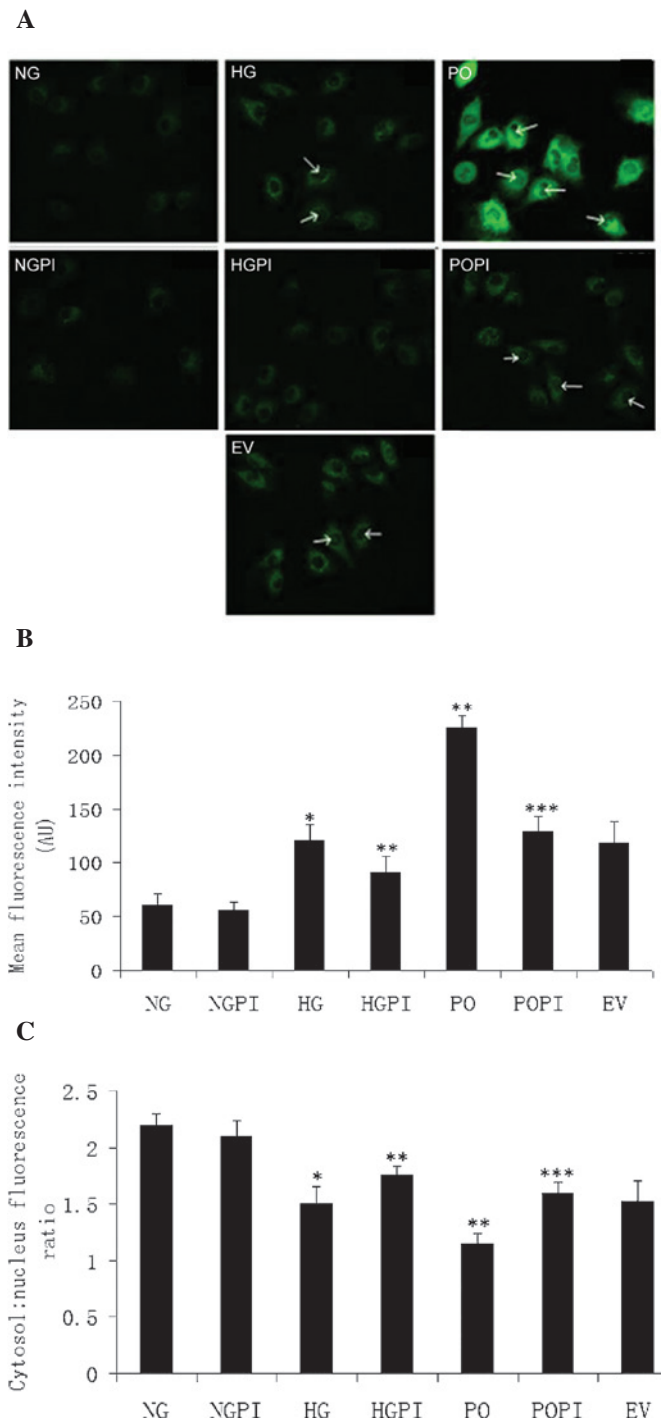


Figure 6. Determination of fluorescence intensity. (A) Expression and distribution of NF- κ B (p65/RELA), determined using confocal microscopy (magnification, $\times 400$) in the seven treatment groups: Normal glucose control group (5.6 mmol/l glucose); high glucose group (25 mmol/l glucose); empty vector control (25 mmol/l glucose+Ad5-null); PKC- β_2 overexpression (25 mmol/l glucose+Ad5-PKC- β_2); PKC- β_2 inhibition (25 mmol/l glucose+Ad5-PKC- β_2 +1 μ mol/l CGP53353); high glucose inhibition (25 mmol/l glucose+1 μ mol/l CGP53353); normal glucose inhibition (5.6 mmol/l glucose+1 μ mol/l CGP53353). Green fluorescence represents protein abundance of p65/RELA in the HUVECs. White arrows indicate increased fluorescence in the nucleus. (B) Mean fluorescence intensity in the cells. (C) Measurement of the cytosol: nucleus fluorescence ratio. The error bars represent the mean \pm standard deviation of the mean. * $P<0.05$, vs. NG control group; ** $P<0.05$, vs. HG group; *** $P<0.05$, vs. PO group ($n=5$). HUVECs, human umbilical vein endothelial cells; RELA, v-rel avian reticuloendotheliosis viral oncogene homolog A; PKC- β_2 , protein kinase C- β_2 ; NG, normal glucose group; HG, high glucose group; EV, empty vector group; PO, PKC- β_2 overexpression group; POPI, PKC- β_2 inhibition group; HGPI, high glucose inhibition group; NGPI, normal glucose inhibition group.

Table III. Cell cycle distribution in various experimental groups.

Group	G ₀ /G ₁ (%)	S (%)	G ₂ /M (%)
NG	68.51±2.08	20.55±3.21	10.95±2.36
HG	73.78±3.85 ^a	22.15±2.42 ^a	4.07±1.21 ^a
EV	72.06±2.18	23.45±3.02	3.49±2.20
PO	40.98±3.86 ^b	38.23±4.33 ^b	22.42±1.68 ^b

^aP<0.05, HG vs NG; ^bP<0.05, PO vs HG. Values are expressed as the mean ± standard error (n=3). Groups: NG, normal glucose group; HG, high-glucose group; EV, empty vector control group; PO, protein kinase C- β_2 overexpression group.

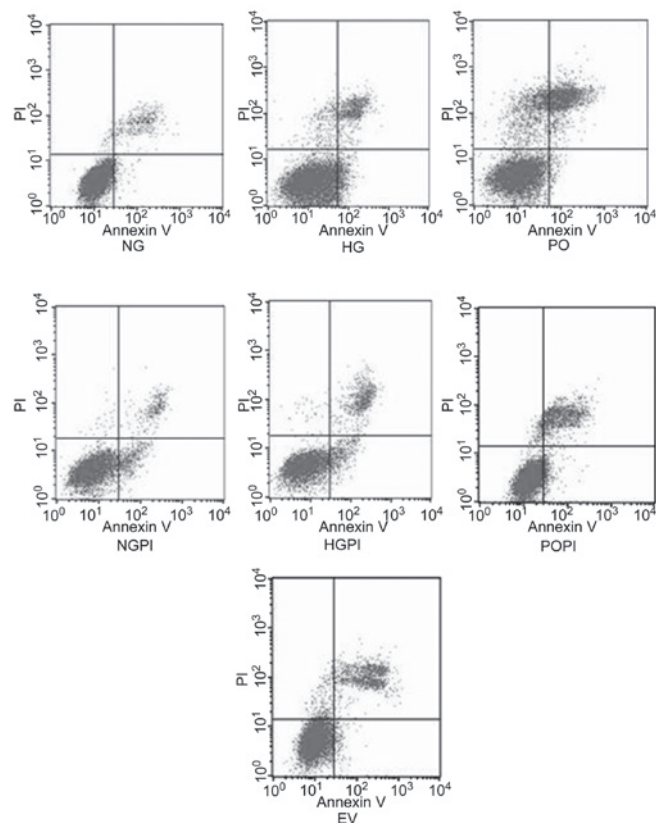


Figure 7. HUVECs were treated according to the following treatment groups: Normal glucose control group (5.6 mmol/l glucose); high glucose group (25 mmol/l glucose); empty vector control group (25 mmol/l glucose+Ad5-null); PKC- β_2 overexpression group (25 mmol/l glucose+Ad5-PKC- β_2); a PKC- β_2 inhibition group (25 mmol/l glucose+Ad5-PKC- β_2 +1 μ mol/l CGP53353); high glucose inhibition group (25 mmol/l glucose+1 μ mol/l CGP53353); normal glucose inhibition group (5.6 mmol/l glucose+1 μ mol/l CGP53353). Cytogram of the cells undergoing apoptosis demonstrates the early apoptotic cells in the lower right quadrant, which were Annexin V positive and phosphatidyl inositol negative. Late apoptotic or necrotic cells are in the upper right quadrant, which were phosphatidyl inositol positive and Annexin V positive. Live cells in the lower left quadrant were negative for the two fluorescent probes. HUVECs, human umbilical vein endothelial cells; PKC- β_2 , protein kinase C- β_2 ; NG, normal glucose group; HG, high glucose group; EV, empty vector group; PO, PKC- β_2 overexpression group; POPI, PKC- β_2 inhibition group; HGPI, high glucose inhibition group; NGPI, normal glucose inhibition group; PI, propidium iodide.

G₀/G₁ phase in the NG, HG and EV groups (Table III). By contrast, high glucose (25 mmol/l) induced cell cycle arrest in the G₀/G₁ phase, compared with normal glucose (P<0.05). The distribution of endothelial cells throughout the phases

of the cell cycle when exposed to high glucose, and overexpressing Ad5-PKC- β_2 (PO group) was 40.98±3.86% for the G₀/G₁ phase, 38.23±4.33% for the S phase and 22.42±1.68% for the G₂/M phase. The percentage of cells in the S and G₂/M phases increased significantly when the cells were transfected with Ad5-PKC- β_2 , compared with the high glucose control (P<0.05). No significant difference was observed in the EV cells exposed to 25 mmol/l glucose, compared with the HG group (P>0.05).

Growth studies. The growth conditions of the cells were detected using flow cytometric analysis. The results demonstrated that ~4.9±0.98% of the cells underwent early apoptosis in response to 5.6 mmol/l glucose exposure for six days, whereas ~8.70±1.15% of the cells were considered early apoptotic in the presence of 25 mmol/l glucose. The early apoptosis ratio of the cells exposed to 25 mmol/l glucose was increased by 1.78-fold, compared with that of the cells exposed to 5.6 mmol/l glucose (Fig. 7; P<0.05). However, the early apoptosis ratio of cells overexpressing PKC- β_2 exposed to 25 mmol/l glucose was markedly decreased (73.8±5.23%), compared with the HG group (P<0.05). By contrast, the cells transfected either with or without the Ad5-null empty vector, and cultured under conditions of high glucose exhibited no significant changes in apoptotic ratio distribution (P>0.05). To examine whether PKC- β_2 modulated high glucose-induced cell cycle acceleration and proliferation, the cells were also treated with a PKC- β_2 selective inhibitor, CGP53353 (1 μ mol/l), which amplified the anti-proliferative and pro-apoptotic effects of high glucose exposure in the cultured HUVECs. These results suggested that the overexpression of PKC- β_2 led to cell cycle acceleration and proliferation, whereas inhibition of the PKC- β_2 isoform had the reverse effect (P<0.05).

Network of PKC- β_2 -associated proteins, determined using subcellular proteomics. A human PPI network of potential connections was determined for the PKC- β_2 -associated proteins identified in the proteomics investigation, using BioGRID 3.1. Among the 50 proteins identified by MALDI-TOF-MS, 14 exhibited successful connections (Fig. 8). These were involved in inflammation, proliferation, cell cycle, apoptosis and cellular metabolism. These results were based on predictions and relevant reports, and provide a novel technique to identify intracellular crosstalk and potential cellular signaling pathways associated with PKC- β_2 .

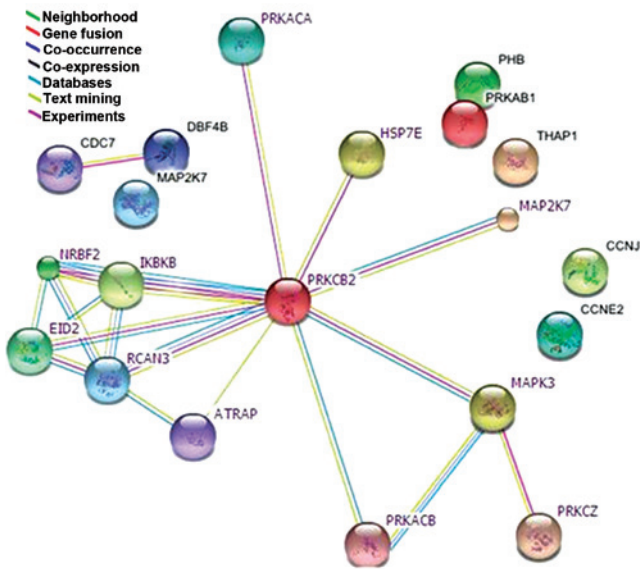


Figure 8. Human protein-protein interaction network in human umbilical vein endothelial cells from the biological general repository for interaction datasets (BioGRID 3.1).

Discussion

The present study established an *in vitro* cell model of constitutively active PKC- β_2 in HUVECs exposed to high ambient glucose levels, which imitated the critical molecular events of diabetes-associated vascular complications. The results of the present study confirmed the effectiveness of recombinant adenovirus transfection of HUVECs using immunoblotting. A subcellular proteomics-based approach was undertaken to profile the alterations in the molecular events in the nuclear and cytoplasmic fractions of endothelial cells prior to, and following, PKC- β_2 activation. The present study focused, not only on the differential protein expression in HUVECs in response to high glucose conditions, but also on the effectors induced by sustained PKC- β_2 activity. A total of 50 proteins were identified by MALDI-TOF-MS and exhibited variation in concentration in response to constitutive PKC- β_2 activation. The proteins were associated with biosynthesis, metabolism, cell cycle, apoptosis, proliferation transcription and translation, and were associated with the protein kinase family. Among the identified proteins associated with PKC- β_2 were important effector proteins: PPAR- δ , NKIRAS1, mitogen-activated protein kinase 3 (MAPK3), cell division cycle 7-related protein kinase (CDC7) and protein DBF4 homolog B (DBF4B; listed in Table II), which are involved in glucose metabolism crosstalk, lipid metabolism crosstalk, inflammatory response, cell proliferation and cell cycle alterations, respectively. The identification of PPAR- δ and NKIRAS1 were further demonstrated using western blot analyses. In addition, to determine the role of high glucose levels and constitutively active PKC- β_2 in the potential PKC- β_2 -NF- κ B inhibitor (I κ B)-NF- κ B signaling pathway in HUVECs, protein function was analyzed. The characteristics and results for each protein are discussed below.

Inflammatory response: NKIRAS1. NF- κ B is a well-known transcription factor that directly regulates the expression of

immediate-early genes and genes involved in the inflammatory response following physiological or pathological stimuli, including high glucose stress (28,29). As previously reported, cells exposed to high glucose, and vascular tissues from patients with diabetes exhibit increased NF- κ B activity (30). The activation of NF- κ B may function as a causal event in intracellular inflammation and endothelial cell dysfunction (31). Kouroedov *et al* (32) demonstrated that glucose-induced phosphorylation of PKC- β_2 activated NF- κ B via an I κ B α -dependent mechanism. However, I κ B α /I κ B β is less resistant to degradation under high glucose stress (33), and the role of PKC- β_2 in glucose-induced NF- κ B activation in arterial endothelial cells remains to be fully elucidated. NKIRAS1 is an atypical Ras-like protein, which acts as a potent regulator of NF- κ B activity by inhibiting the phosphorylation of I κ B and mediating the cytoplasmic retention of the p65/RELA NF- κ B subunit (27). NKIRAS1 interacts with I κ B α and I κ B β *in vitro*, however, it has rarely been reported as an important intermediate in tissue biology, and the only available study focused on its role in human renal cell carcinomas (34). The results of the present study demonstrated a decrease in the cytosolic localization of NKIRAS1 in response to high glucose and sustained PKC- β_2 . Furthermore, treatment of the cells with the selective PKC- β_2 inhibitor CGP53353 inhibited the PKC- β_2 -induced decreased expression of NKIRAS1. Based on these results, it was hypothesized that high glucose-induced activation of PKC- β_2 led to a decrease of NKIRAS1 in the cytoplasm, and that this alteration induced I κ B α /I κ B β degradation resistance. As a result, NF- κ B and the I κ B-bound complex were inclined to disaggregate and, simultaneously, an NF- κ B subunit, including p65/RELA entered the nucleus and activated gene expression. To verify this hypothesis, further investigations were performed. Glucose-induced upregulation and nuclear translocation of NF- κ B (p65/RELA) were predominantly prevented by the selective inhibition of PKC- β_2 . The decrease in the cytosolic localization of NKIRAS1 explained the increased rate of I κ B α /I κ B β degradation and the nuclear translocation of NF- κ B (p65/RELA) in HUVECs exposed to high ambient glucose. Thus, the present study identified a potential PKC- β_2 -I κ B-NF- κ B signaling pathway in HUVECs under conditions of high glucose. The data further suggested that NKIRAS1 may be an important modulator of NF- κ B activity, by regulating the interaction between I κ B and NF- κ B.

Glucose and lipid metabolism crosstalk: PPAR- δ . In the present study, another protein that exhibited changes in expression was PPAR- δ . PPAR- δ is a member of the PPAR family, and PPARs are ligand-activated transcription factors that regulate the expression of genes involved in fatty acid uptake and oxidation, lipid metabolism and inflammation (35,36). The three PPAR subtypes, PPAR- α , PPAR- γ and PPAR- δ (or PPAR- β), have distinct tissue distributions and functions. PPAR- α and PPAR- γ are predominantly expressed in liver and adipose tissue, respectively, whereas PPAR- δ is ubiquitously expressed (37). Several studies have suggested PPAR- δ has important metabolic regulatory functions (38). PPAR- δ increases fatty acid oxidation in adipocytes (39), augments lipogenesis and glycolysis in the liver (40) and increases oxidative metabolism in skeletal muscles (41,42). However, its physiological and pathophysiological roles in endothelial cells, which are critical in vascular

biology, remain to be fully elucidated. In the present study, high glucose-induced upregulation in the expression of PPAR- δ was observed in the HUVECs. These results are concordant with those of a previous study on vascular endothelial cells (VECs) by Riahi *et al* (43), who reported that PPAR- δ is the endogenous receptor activated under hyperglycemic conditions in VECs and demonstrated that high glucose levels inhibit glucose transport and total glucose transporter-1 expression levels in a PPAR- δ -dependent manner. Kim *et al* (44) also determined that 25 mmol/l glucose increases the gene expression of PPAR- δ in mouse embryonic stem cells. The results of the present study demonstrated a decrease in the nuclear localization of PPAR- δ in response to constitutively active PKC- β_2 , as determined by western blot analyses. These results were concordant with those obtained from the 2-DE analysis, demonstrating that the quantitative change of PPAR- δ is, in part, associated with excessive activation of the PKC- β_2 isoform. This hypothesis was further supported by the use of the PKC- β_2 inhibitor, CGP53353. To the best of our knowledge, PPAR- δ has yet to be reported as a functional downstream effector of PKC- β_2 signaling. Although the underlying mechanism remains to be elucidated, PKC- β_2 may be involved in glucose and lipid metabolism crosstalk by regulating PPAR- δ . Further investigation is required in order to reveal the mechanisms underlying this association.

Molecular events of cell proliferation and the cell cycle: MAPK3, DBF4B and CDC7. Previous studies have demonstrated that high glucose levels affect vascular endothelial cell proliferation, however, the role of PKC isoforms in cell proliferation remains to be fully elucidated (45-47). Flow cytometric analysis was used to determine which phase of the cell cycle was affected by high glucose exposure, as well as the effect PKC- β_2 had on cell proliferation and the cell cycle. The results indicated that overexpression of PKC- β_2 promoted cell proliferation by reducing early apoptosis and increased the percentage of cells in the S and G₂/M phases under high glucose conditions in HUVECs. Neri *et al* (48) reported that the oral protein-kinase C beta inhibitor enza-staurin (LY317615) inhibits proliferation by suppressing signaling via the Akt pathway in multiple myeloma cell lines. However, the potential signaling mechanism underlying the PKC- β_2 -induced enhancement of endothelial cell proliferation remains to be elucidated. In the present study 2-DE analysis revealed that the overexpression of PKC- β_2 led to an increase in the expression of MAPK3, the activation of which is important in the development of diabetic vascular complications. The expression levels of MAPK3, also termed ERK1 and p44-MAPK, were also quantitatively changed, as observed using MALDI-TOF-MS. MAPK3 is activated by upstream kinases, resulting in its translocation to the nucleus where it phosphorylates nuclear targets (49). Yang *et al* (50) reported that activated MAPK3/1 activates PKC via phospholipase A2 group IVA, and activated PKC further stimulates MAPK3/1 via the reactivation of raf-1 proto-oncogene serine/threonine kinase and MAP2K1. MAPK3 acts in a signaling cascade that regulates various cellular processes, including proliferation, differentiation and cell cycle progression (51). In the PPI network in the present study, MAPK3 was associated with PKC- β_2 signaling, suggesting that it may be involved in PKC- β_2 -induced cell proliferation under

high glucose conditions in HUVECs. This signal amplification and the potential for crosstalk appear to be important features of the PKC- β_2 signaling pathway, however, the activation of MAPK3 in the PKC- β_2 signaling pathway was not an isolated molecular event. DBF4B and CDC7 are cell cycle regulatory proteins, and their expression levels were quantitatively altered in response to PKC- β_2 activation using MS. As determined from the PPI network, the DBF4B and CDC7 proteins interacted. Previous studies have demonstrated that the CDC7-DBF4 complex is involved in regulating the initiation of DNA replication during cell cycle progression (52,53). Specifically, the complex is required for the progression of the cells between the S and M phase. Flow cytometric analysis demonstrated that activation of PKC- β_2 led to a rapid increase in the number of cells in the S/M phase of the cell cycle, and markedly increased the rate of mitosis. The upregulation in the expression of CDC7-DBF4 may partly explain the cell cycle alterations induced by PKC- β_2 signaling. The results of the proteomics investigation suggested that MAPK3, DBF4B and CDC7 may act downstream of PKC- β_2 . However, further investigations are required in order to elucidate the mechanisms underlying the dominant roles of these proteins in the maintaining the balance between cell death and survival.

PPI networks. Proteins in a 'subproteome' are expected to exhibit apparent function-dependent associations. To examine a PPI network of the potential connections for PKC- β_2 -associated proteins in the present study, the identified proteins were entered into BioGRID 3.1, a protein network and pathway analysis algorithm. A total of 36 molecules from the dataset exhibited no association with any other molecules in the group, which may have occurred due to limitations of the database and article searches, or due to the novelty of the proteins in this network. Therefore, further investigations on the biological processes and underlying molecular functions of these molecules are required to evaluate whether they require inclusion in the network.

To the best of our knowledge, the present study is the first to use subcellular and functional proteomics to profile subcellular signaling in endothelial cells prior to, and following, PKC- β_2 activation. The proteomics analysis provided a detailed profile of these changes at the molecular level, and a number of the altered proteins identified were consistent with those of previous studies (54-56). The results of the present study demonstrated that PKC- β_2 may be an important molecular regulator of high glucose-induced functional and metabolic changes in HUVECs. The data further suggested that PKC- β_2 may be involved in glucose and lipid metabolism crosstalk, inflammatory response, cell proliferation and alterations in the cell cycle. PKC- β_2 may be involved in high glucose-induced glucose and lipid crosstalk by regulating PPAR- δ . In addition, NKIRAS1 may be important in a potential PKC- β_2 -I κ B-NF- κ B signaling pathway in HUVECs under high glucose conditions. The present study enhanced the current understanding of the molecular mechanisms underlying PKC- β_2 -stimulated cross-talk in the signaling pathways involved in pathophysiological conditions associated with diabetic vascular complications. The results of the present study indicated that PKC- β_2 is a promising potential target for the treatment of vascular complications

of diabetes. Clinical treatments targeting key signaling molecules of the PKC- β 2 pathway may achieve remissions of diabetes-associated vascular diseases or prevent common medical complications in diabetic patients.

Acknowledgements

The present study was supported by the National Natural Science Foundation of China (grant nos. 30570877 and 81370940) and the National Key Clinical Department Construction Project. The authors of the present study acknowledge the support of the Ophthalmology Laboratory of Chongqing Medical University, and are grateful to Dr Mingjun Wu for the MALDI-TOF-MS analysis and to Dr Yongbo Peng for technological support with the PPI network.

References

- Yang W, Lu J, Weng J, Jia W, Ji L, Xiao J, Shan Z, Liu J, Tian H, Ji Q, *et al*: Prevalence of diabetes among men and women in China. *N Engl J Med* 362: 1090-1101, 2010.
- Bakker W, Eringa EC, Sipkema P and van Hinsbergh VW: Endothelial dysfunction and diabetes: Roles of hyperglycemia, impaired insulin signaling and obesity. *Cell Tissue Res* 335: 165-189, 2009.
- Orasanu G and Plutzky J: The pathologic continuum of diabetic vascular disease. *J Am Coll Cardiol* 53 (5 Suppl): S35-S42, 2009.
- Yuan SY, Ustinova EE, Wu MH, Tinsley JH, Xu W, Korompai FL and Taulman AC: Protein kinase C activation contributes to microvascular barrier dysfunction in the heart at early stages of diabetes. *Circ Res* 87: 412-417, 2000.
- King GL: The role of hyperglycaemia and hyperinsulinaemia in causing vascular dysfunction in diabetes. *Ann Med* 28: 427-432, 1996.
- Hink U, Li H, Mollnau H, Oelze M, Matheis E, Hartmann M, Skatchkov M, Thaiss F, Stahl RA and Warnholtz A: Mechanisms underlying endothelial dysfunction in diabetes mellitus. *Circ Res* 88: E14-E22, 2001.
- Kizub IV, Klymenko KI and Soloviev AI: Protein kinase C in enhanced vascular tone in diabetes mellitus. *Int J Cardiol* 174: 230-242, 2014.
- Geraldes P and King GL: Activation of protein kinase C isoforms and its impact on diabetic complications. *Circ Res* 106: 1319-1331, 2010.
- Meier M, Park JK, Overheu D, Kirsch T, Lindschau C, Gueler F, Leitges M, Menne J and Haller H: Deletion of protein kinase C-beta isoform in vivo reduces renal hypertrophy but not albuminuria in the streptozotocin-induced diabetic mouse model. *Diabetes* 56: 346-354, 2007.
- Gaudreault N, Perrin RM, Guo M, Clanton CP, Wu MH and Yuan SY: Counter regulatory effects of PKCbetaII and PKCdelta on coronary endothelial permeability. *Arterioscler Thromb Vasc Biol* 28: 1527-1533, 2008.
- Dangwal S, Rauch BH, Gensch T, Dai L, Bretschneider E, Vogelaar CF, Schrör K and Rosenkranz AC: High glucose enhances thrombin responses via protease-activated receptor-4 in human vascular smooth muscle cells. *Arterioscler Thromb Vasc Biol* 31: 624-633, 2011.
- Naruse K, Rask-Madsen C, Takahara N, Ha SW, Suzuma K, Way KJ, Jacobs JR, Clermont AC, Ueki K, Ohshiro Y, *et al*: Activation of vascular protein kinase C-beta inhibits Akt-dependent endothelial nitric oxide synthase function in obesity-associated insulin resistance. *Diabetes* 55: 691-698, 2006.
- Lin X, Zhou B and Sun F: Protein Kinase C β 2 mediated high glucose-induced human umbilical vein endothelial cells injury via regulation of peroxisome proliferator-activated receptor α . *China J Endocrinol Metab* 26: 10-14, 2010.
- Min W, Bin ZW, Quan ZB, Hui ZJ and Sheng FG: The signal transduction pathway of PKC/NF-kappa B/c-fos may be involved in the influence of high glucose on the cardiomyocytes of neonatal rats. *Cardiovasc Diabetol* 8: 8, 2009.
- Campbell M and Trimble ER: Modification of PI3K- and MAPK-dependent chemotaxis in aortic vascular smooth muscle cells by protein kinase CbetaII. *Circ Res* 96: 197-206, 2005.
- Duan L, Lin XB and Zhou B: Construction and identification of endothelial cell model with overexpressed human protein kinase C β 2 induced by high glucose. *Acta Acad Med Militaris Tertiae* 31: 1993-1996, 2009 (In Chinese).
- Sun F, Zhou B, Lin X and Duan L: Proteomic analysis identifies nuclear protein effectors in PKC- δ signaling under high glucose-induced apoptosis in human umbilical vein endothelial cells. *Mol Med Rep* 4: 865-872, 2011.
- Turck N, Richert S, Gendry P, Stutzmann J, Kedinger M, Leize E, Simon-Assmann P, Van Dorsselaer A and Launay JF: Proteomic analysis of nuclear proteins from proliferative and differentiated human colonic intestinal epithelial cells. *Proteomics* 4: 93-105, 2004.
- Cargnello M and Roux PP: Activation and function of the MAPKs and their substrates, the MAPK-activated protein kinases. *Microbiol Mol Biol Rev* 75: 50-83, 2011.
- Furukohri A, Sato N, Masai H, Arai K, Sugino A and Waga S: Identification and characterization of a *Xenopus* homolog of Dbf4, a regulatory subunit of the Cdc7 protein kinase required for the initiation of DNA replication. *J Biochem* 134: 447-457, 2003.
- Jiang W, McDonald D, Hope TJ and Hunter T: Mammalian Cdc7-Dbf4 protein kinase complex is essential for initiation of DNA replication. *EMBO J* 18: 5703-5713, 1999.
- Kim JM, Sato N, Yamada M, Arai K and Masai H: Growth regulation of the expression of mouse cDNA and gene encoding a serine/threonine kinase related to *Saccharomyces cerevisiae* CDC7 essential for G1/S transition. Structure, chromosomal localization, and expression of mouse gene for *S. cerevisiae* Cdc7-related kinase. *J Biol Chem* 273: 23248-23257, 1998.
- Jares P, Luciani MG and Blow JJ: A *xenopus* Dbf4 homolog is required for Cdc7 chromatin binding and DNA replication. *BMC Mol Biol* 5: 5, 2004.
- Monsalve FA, Pyarasani RD, Delgado-Lopez F and Moore-Carrasco R: Peroxisome proliferator-activated receptor targets for the treatment of metabolic diseases. *Mediators Inflamm* 2013: 549627, 2013.
- Saez ME, Grilo A, Moron FJ, Manzano L, Martínez-Larrad MT, Gonzalez-Perez A, Serrano-Hernando J, Ruiz A, Ramirez-Lorca R and Serrano-Rios M: Interaction between calpain 5, peroxisome proliferator-activated receptor-gamma and peroxisome proliferator-activated receptor-delta genes: A polygenic approach to obesity. *Cardiovasc Diabetol* 7: 23, 2008.
- Mosser DD, Caron AW, Bourget L, Denis-Larose C and Massie B: Role of the human heat shock protein hsp70 in protection against stress-induced apoptosis. *Mol Cell Biol* 17: 5317-5327, 1997.
- Lin H, Wang Y, Zhang X, Liu B, Zhang W and Cheng J: Prognostic significance of kappaB-Ras expression in gliomas. *Med Oncol* 29: 1272-1279, 2012.
- Jeong IK, Oh da H, Park SJ, Kang JH, Kim S, Lee MS, Kim MJ, Hwang YC, Ahn KJ, Chung HY, *et al*: Inhibition of NF- κ B prevents high glucose-induced proliferation and plasminogen activator inhibitor-1 expression in vascular smooth muscle cells. *Exp Mol Med* 43: 684-692, 2011.
- Green CJ, Pedersen M, Pedersen BK and Scheele C: Elevated NF- κ B activation is conserved in human myocytes cultured from obese type 2 diabetic patients and attenuated by AMP-activated protein kinase. *Diabetes* 60: 2810-2819, 2011.
- Chen S, Khan ZA, Cukiernik M and Chakrabarti S: Differential activation of NF-kappaB and AP-1 in increased fibronectin synthesis in target organs of diabetic complications. *Am J Physiol Endocrinol Metab* 284: E1089-E1097, 2003.
- Csiszar A, Wang M, Lakatta EG and Ungvari Z: Inflammation and endothelial dysfunction during aging: Role of NF-kappaB. *J Appl Physiol* (1985) 105: 1333-1341, 2008.
- Kouroedov A, Eto M, Joch H, Volpe M, Lüscher TF and Cosentino F: Selective inhibition of protein kinase Cbeta2 prevents acute effects of high glucose on vascular cell adhesion molecule-1 expression in human endothelial cells. *Circulation* 110: 91-96, 2004.
- Tang JR, Michaelis KA, Nozik-Grayck E, Seedorf GJ, Hartman-Filson M, Abman SH and Wright CJ: The NF- κ B inhibitory proteins I κ B α and I κ B β mediate disparate responses to inflammation in fetal pulmonary endothelial cells. *J Immunol* 190: 2913-2923, 2013.
- Gerashchenko GV, Bogatyrova OO, Rudenko EE, Kondratov AG, Gordiyuk VV, Zgonnyk YM, Vozianov OF, Pavlova TV, Zabarovsky ER, Rynditch AV and Kashuba VI: Genetic and epigenetic changes of NKIRAS1 gene in human renal cell carcinomas. *Exp Oncol* 32: 71-75, 2010.

35. Duan SZ, Usher MG and Mortensen RM: PPARs: The vasculature, inflammation and hypertension. *Curr Opin Nephrol Hypertens* 18: 128-133, 2009.
36. Wahli W and Michalik L: PPARs at the crossroads of lipid signaling and inflammation. *Trends Endocrinol Metab* 23: 351-363, 2012.
37. Escher P, Braissant O, Basu-Modak S, Michalik L, Wahli W and Desvergne B: Rat PPARs: Quantitative analysis in adult rat tissues and regulation in fasting and refeeding. *Endocrinology* 142: 4195-4202, 2001.
38. Reilly SM and Lee CH: PPAR delta as a therapeutic target in metabolic disease. *FEBS Lett* 582: 26-31, 2008.
39. Wang YX, Lee CH, Tiep S, Yu RT, Ham J, Kang H and Evans RM: Peroxisome-proliferator-activated receptor delta activates fat metabolism to prevent obesity. *Cell* 113: 159-170, 2003.
40. Lee CH, Olson P, Hevener A, Mehl I, Chong LW, Olefsky JM, Gonzalez FJ, Ham J, Kang H, Peters JM and Evans RM: PPARdelta regulates glucose metabolism and insulin sensitivity. *Proc Natl Acad Sci USA* 103: 3444-3449, 2006.
41. Luquet S, Lopez-Soriano J, Holst D, Fredenrich A, Melki J, Rassoulzadegan M and Grimaldi PA: Peroxisome proliferator-activated receptor delta controls muscle development and oxidative capability. *FASEB J* 17: 2299-2301, 2003.
42. Wang YX, Zhang CL, Yu RT, Cho HK, Nelson MC, Bayuga-Ocampo CR, Ham J, Kang H and Evans RM: Regulation of muscle fiber type and running endurance by PPARdelta. *PLoS Biol* 2: e294, 2004.
43. Riahi Y, Sin-Malia Y, Cohen G, Alpert E, Gruzman A, Eckel J, Staels B, Guichardant M and Sasson S: The natural protective mechanism against hyperglycemia in vascular endothelial cells: Roles of the lipid peroxidation product 4-hydroxydodecadienal and peroxisome proliferator-activated receptor delta. *Diabetes* 59: 808-818, 2010.
44. Kim YH and Han HJ: High-glucose-induced prostaglandin E (2) and peroxisome proliferator-activated receptor delta promote mouse embryonic stem cell proliferation. *Stem Cells* 26: 745-755, 2008.
45. Keats E and Khan ZA: Unique responses of stem cell-derived vascular endothelial and mesenchymal cells to high levels of glucose. *PLoS One* 7: e38752, 2012.
46. Yuan L, Hu J, Luo Y, Liu Q, Li T, Parish CR, Freeman C, Zhu X, Ma W, Hu X, *et al*: Upregulation of heparanase in high-glucose-treated endothelial cells promotes endothelial cell migration and proliferation and correlates with Akt and extra-cellular-signal-regulated kinase phosphorylation. *Mol Vis* 18: 1684-1695, 2012.
47. Su J, Zhou H, Tao Y, Guo J, Guo Z, Zhang S, Zhang Y, Huang Y, Tang Y, Dong Q and Hu R: G-CSF protects human brain vascular endothelial cells injury induced by high glucose, free fatty acids and hypoxia through MAPK and Akt signaling. *PLoS One* 10: e0120707, 2015.
48. Neri A, Marmiroli S, Tassone P, Lombardi L, Nobili L, Verdelli D, Civallero M, Cosenza M, Bertacchini J, Federico M, *et al*: The oral protein-kinase C beta inhibitor enzastaurin (LY317615) suppresses signalling through the AKT pathway, inhibits proliferation and induces apoptosis in multiple myeloma cell lines. *Leuk Lymphoma* 49: 1374-1383, 2008.
49. Caunt CJ and McArdle CA: ERK phosphorylation and nuclear accumulation: Insights from single-cell imaging. *Biochem Soc Trans* 40: 224-229, 2012.
50. Yang P and Roy SK: A novel mechanism of FSH regulation of DNA synthesis in the granulosa cells of hamster preantral follicles: Involvement of a protein kinase C-mediated MAP kinase 3/1 self-activation loop. *Biol Reprod* 75: 149-157, 2006.
51. Winnicki K, Zabka A, Bernasinska J, Matczak K and Maszewski J: Immunolocalization of dually phosphorylated MAPKs in dividing root meristem cells of *Vicia faba*, *Pisum sativum*, *Lupinus luteus* and *Lycopersicon esculentum*. *Plant Cell Rep* 34: 905-917, 2015.
52. Hiraga S, Alvino GM, Chang F, Lian HY, Sridhar A, Kubota T, Brewer BJ, Weinreich M, Raghuraman MK and Donaldson AD: Rif1 controls DNA replication by directing protein phosphatase 1 to reverse Cdc7-mediated phosphorylation of the MCM complex. *Genes Dev* 28: 372-383, 2014.
53. Yamada M, Watanabe K, Mistrik M, Vesela E, Protivankova I, Mailand N, Lee M, Masai H, Lukas J and Bartek J: ATR-Chk1-APC/CCdh1-dependent stabilization of Cdc7-ASK (Dbf4) kinase is required for DNA lesion bypass under replication stress. *Genes Dev* 27: 2459-2472, 2013.
54. Zhao Y, Zhang Y, Song HB, Wu F, Wang XL, Sun SC, Cui TX and Tang DQ: Proteomic analysis revealed the altered kidney protein profile of a Cylid knockout mouse model. *Genet Mol Res* 14: 5970-5978, 2015.
55. Pizzatti L, Sa LA, de Souza JM, Bisch PM and Abdelhay E: Altered protein profile in chronic myeloid leukemia chronic phase identified by a comparative proteomic study. *Biochim Biophys Acta* 1764: 929-942, 2006.
56. Ezkurdia I, del Pozo A, Frankish A, Rodriguez JM, Harrow J, Ashman K, Valencia A and Tress ML: Comparative proteomics reveals a significant bias toward alternative protein isoforms with conserved structure and function. *Mol Biol Evol* 29: 2265-2283, 2012.